JOURNAL OF NATURAL PRODUCTS

Article

pubs.acs.org/jnp

ent-Labdane Diterpenoids from the Aerial Parts of *Eupatorium obtusissmum*

Quírico A. Castillo,*[,†,‡] Jorge Triana,[§] José L. Eiroa,[§] Laurent Calcul,[⊥] Edwin Rivera,[⊥,∥] Lukasz Wojtas,[⊥] José M. Padrón,[▽] Lise Boberieth,[⊥] Mehdi Keramane,[○] Ernesto Abel-Santos,[#] Luis A. Báez,[†] and Evelyn A. Germosén[‡]

[†]Escuela de Química and [‡]Instituto de Química, Universidad Autónoma de Santo Domingo (UASD), Facultad de Ciencias, Ciudad Universitaria, Santo Domingo, D.N., Dominican Republic

[§]Departamento de Química, Unidad Asociada al CSIC, Universidad de Las Palmas de Gran Canaria, Campus de Tafira, 35017, Las Palmas de Gran Canaria, Canary Islands, Spain

[⊥]Florida Center of Excellence for Drug Discovery and Innovation (CDDI-USF), University of South Florida, Tampa, Florida 33620, United States

[∥]Department of Chemistry, University of South Florida, 4202 East Fowler Avenue, Tampa, Florida 33612, United States

[▽]BioLab, Instituto Universitario de Bio-Orgánica Antonio González (IUBO-AG), Centro de Investigaciones Biomédicas de Canarias (CIBICAN), Universidad de La Laguna, 38206 La Laguna, Spain

[○]Biointerfaces Institute, McMaster University, Engineering Technology Building, Room 413, 1280 Main Street West, Hamilton, ON L8S 0A3, Canada

[#]Department of Chemistry and Biochemistry, University of Nevada, Las Vegas, Nevada 89154, United States

Supporting Information

ABSTRACT: Six new *ent*-labdane diterpenoids, uasdlabdanes A–F (**1**–**6**), were isolated from the aerial parts of *Eupatorium obtusissmum*. The new structures were elucidated through spectroscopic and spectrometric data analyses. The absolute configurations of compounds **1** and **2** were established by X-ray crystallography, and those of **3**–**6**, by comparison of experimental and calculated electronic circular dichroism spectra. The antiproliferative activity of the compounds was studied in a panel of six representative human solid tumor cell lines and showed GI_{50} values ranging from 19 to >100 μM.

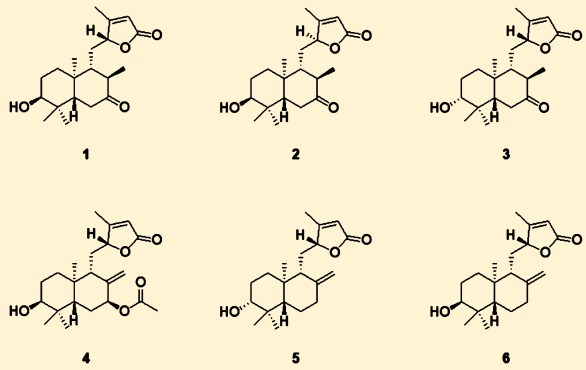

Eupatorium obtusissmum P. DC. (Asteraceae) is an endemic plant from the island of Hispaniola.[1] Following an interest in discovering new and interesting secondary metabolites, a phytochemical study of *E. obtusissmum* was undertaken and led to the identification of six new *ent*-labdane diterpenoids, uasdlabdanes A–F (**1**–**6**).

Labdane-type diterpenoids constitute a large family of natural products and constitute more than 7000 known compounds.[2] They are widely distributed in plants within botanical families, such as the Labiatae, Asteraceae, Acanthaceae, Euphorbiaceae, Chloranthaceae, and Zingiberaceae.[3] Many labdane-type diterpenoids have been reported to have a variety of bioactivities, including antibacterial,[4] cytotoxic,[5] anti-inflammatory,[6] and hepatoprotective[7] activities, as well as neuroprotective effects.[8] Herein, the isolation and structural elucidation of uasdlabdanes A–F (**1**–**6**) and their antiproliferative activities over six human solid tumor cell lines are discussed.

RESULTS AND DISCUSSION

The CH_2Cl_2 fraction (4.4 g) of the ethanolic extract of *E. obtusissmum* yielded uasdlabdanes A (**1**, 22 mg), B (**2**, 0.4 mg), C (**3**, 0.5 mg), D (**4**, 16 mg), E (**5**, 1.0 mg), and F (**6**, 0.5 mg) after several chromatographic procedures.

Uasdlabdane A (**1**) was obtained as colorless crystals. Its molecular formula was assigned as $C_{20}H_{30}O_4$, based on its HRESIMS (*m*/*z* 357.2046 $[M + Na]^+$, calcd 357.2042) and ^{13}C NMR data, indicating six indices of hydrogen deficiency. Its IR spectrum revealed the presence of a hydroxy group (3499 cm^{-1}), a conjugated lactone (1722 cm^{-1}), and a ketocarbonyl group (1700 cm^{-1}).

The ^1H NMR data of **1** are summarized in Table 1 and showed the presence of five methyl groups [δ_H 0.91, 0.95, 1.06,

Received: October 27, 2015
Published: March 29, 2016

DOI: 10.1021/acs.jnatprod.5b00954
J. Nat. Prod. 2016, 79, 907–913

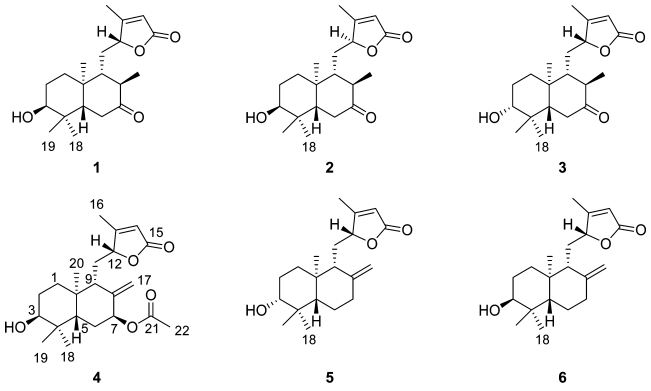

2.09 (s, 3H each) and 1.11 (d, J = 6.36 Hz)], two oxygenated methines [δ_H 3.52 (m) and 4.79 (br d J = 10.8 Hz)], and one olefinic methine [δ_H 5.79 (s)].

The ^{13}C NMR data of **1** are summarized in Table 2. The spectrum showed 20 resonances, including five methyl groups, four methylene carbons, six methine carbons (including one olefinic and two oxygenated), and five quaternary carbons (including one olefinic and two carbonyl).

The partial structures $CH_2(1)-CH_2(2)-CH$ (3), $CH(5)-CH_2(6)$, $CH(8)-CH_3$ (17), and $CH(9)-CH_2(11)-CH(12)$ revealed by the ^{1}H−^{1}H COSY spectrum (Figure 1), as well as the HMBC correlations from H_2-1 (δ_H 1.44, 1.74) to C-10 (δ_C 38.3); from H_2-6 (δ_H 2.36) to C-7 (δ_C 212.0); from H-8 (δ_H 2.14) to C-7; from H-9 (δ_H 1.68) to H-8; from H_3-18 (δ_H 0.91) to H-3 (δ_H 3.52) and C-4 (δ_C 37.7); from H_3-19 (δ_H 0.95) to C-5 (δ_C 46.1) and H_3-18; and from H_3-20 (δ_H 1.06) to C-1 (δ_C 31.6), C-5, C-9 (δ_C 53.2), and C-10 supported the structure of a labdane-type diterpenoid with oxygenation at C-3 and 4,4,8,10-tetramethyl substitutions.

The correlations observed in the ^{1}H−^{1}H COSY spectrum of H-9 (δ_H 1.68)/H-11 (δ_H 2.07), H-11 (δ_H 1.22)/H-12 (δ_H 4.79), and H-12/H-14 (δ_H 5.79) permitted assignment of the furan-2(5*H*)-one structural moiety and its connection to the decalin unit. These assignments were supported by the HMBC correlations from H-14 to C-13 (δ_C 172.6) and C-15 (δ_C 168.3). The assignment of H_3-16 (δ_H 2.09) was evident via its HMBC correlations with C-13 and C-15 and through the correlations with H-12 and H-14 in the ^{1}H−^{1}H COSY spectrum.

The relative configuration of C-18 was determined by the NOESY correlation of H_3-18 with H_3-20. Crystals of **1** were obtained in MeCN−H_2O and facilitated assignment of its absolute configuration as (3*S*, 5*S*, 8*R*, 9*R*, 10*S*, 12*R*) (Figure 2) based on the anomalous scattering signal in the X-ray diffraction data using the Flack approach[9] and subsequently confirmed through Bijvoet-pair analysis and Bayesian statistics.[10] The data have been collected using Cu Kα radiation (λ = 1.541 78 Å) to increase the anomalous dispersion signal as compared to data collected with molybdenum radiation. The Bijvoet-pair analysis and Bayesian statistics have been performed using the program Platon.[11] Thus, the structure was unambiguously identified as an *ent*-labdane diterpenoid and named uasdlabdane A.

Table 1. ^{1}H NMR Data of Compounds 1−6 ($CDCl_3$, δ_H in ppm, J in Hz)

position	1[a]	2[a]	3[b]	4[a]	5[c]	6[a]
1	1.44, m	1.40, m	1.45, m	1.42, m	1.44, m	1.44, m
	1.74, m	1.69, m	1.76, m	1.66, m	1.64, m	1.63, m
2	1.70, m	1.66, m	1.70, m	1.68, m	1.68, m	1.65, m
	1.97, m	1.93, m	1.99, m	1.94, m	1.95, m	1.96, m
3	3.52, m	3.50, br s	3.53, br s	3.46, t (2.5)	3.46, br s	3.46, m
5	1.91, dd (4.7, 13.5)	1.92, m	1.91, dd (4.2, 13.9)	2.01, dd (2.9, 13.6)	1.64, m	1.63, m
6	2.36, m	2.35, m	2.35, m	1.63, m	1.41, br dd (4.2, 12.9)	1.67, m
	2.36, m	2.38, m	2.39, m	1.87, m	1.68, m	1.67, m
7				5.44, t (2.7)	2.05, m	2.05, m
					2.46, br d (12.9)	2.46, m
8	2.14, m	2.35, m	2.15, m			
9	1.68, m	1.69, m	1.71, m	2.37, br d (9.9)	1.97, s	1.97, m
11	1.22, dd (2.9, 4.9)	1.63, m	1.24, m	1.90, m	1.86, m	1.86, m
	2.07, m		2.08, m		1.97, s	1.96, m
12	4.79, br d (10.8)	4.77, br d (10.9)	4.80 br d (10.8)	4.81, m	4.82, m	4.82, m
14	5.79, s	5.81, s	5.80, s	5.75, s	5.75, s	5.75, m
16	2.09, s	2.10, s	2.10, s	2.09, s	2.11, s	2.10, s
17	1.11, d (6.4)	1.19, d (6.8)	1.14, d (6.6)	4.94, d (1.1)	4.71, s	4.71, s
				5.27, s	4.94, s	4.94, s
18	0.91, s	0.89, s	0.96, s	0.82, s	0.86, s	0.85, s
19	0.95, s	0.96, s	0.92, s	0.92, s	0.99, s	0.98, s
20	1.06, s	0.99, s	1.07, s	0.71, s	0.72, s	0.72, s
22				2.05, s		

[a]500 MHz. [b]800 MHz. [c]700 MHz.

DOI: 10.1021/acs.jnatprod.5b00954
J. Nat. Prod. 2016, 79, 907−913

Table 2. ^{13}C NMR Data of Compounds 1−6 ($CDCl_3$, δ_C in ppm)

position	1[a]	2[a]	3[b]	4[a]	5[c]	6[a]
1	31.6, CH_2	30.9, CH_2	31.6, CH_2	31.5, CH_2	31.7, CH_2	31.9, CH_2
2	24.9, CH_2	25.2, CH_2	24.9, CH_2	25.8, CH_2	25.6, CH_2	25.8, CH_2
3	75.1, CH	75.2, CH	75.2, CH	75.5, CH	75.6, CH	75.8, CH
4	37.7, C	38.0, C	38.3, C	37.3, C	37.6, C	37.8, C
5	46.1, CH	46.5, CH	46.1, CH	42.1, CH	48.3, CH	48.5, CH
6	38.1, CH_2	37.9, CH_2	38.1, CH_2	28.6, CH_2	23.7, CH_2	23.9, CH_2
7	212.0, C	211.8, C	211.9, C	75.9, CH	37.8, CH_2	38.0, CH_2
8	47.1, CH	48.4, CH	47.2, CH	144.3, C	147.2, C	147.4, C
9	53.2, CH	53.1, CH	53.2, CH	47.5, CH	52.5, CH	52.7, CH
10	38.3, C	37.6, C	37.7, C	39.5, C	39.5, C	39.7, C
11	32.2, CH_2	33.7, CH_2	32.3, CH_2	27.0, CH_2	27.5, CH_2	27.6, CH_2
12	85.4, CH	84.8, CH	85.4, CH	83.6, CH	84.2, CH	84.4, CH
13	168.3, C	168.3, C	168.1, C	169.2, C	169.2, C	169.5, C
14	117.0, CH	117.1, CH	117.1, CH	116.8, CH	116.3, CH	116.5, CH
15	172.6, C	172.7, C	172.5, C	172.9, C	172.9, C	173.1, C
16	14.1, CH_3	14.0, CH_3	14.1, CH_3	14.8, CH_3	14.6, CH_3	14.8, CH_3
17	13.4, CH_3	13.8, CH_3	13.3, CH_3	113.3, CH_2	107.8, CH_2	108.0, CH_2
18	21.5, CH_3	21.5, CH_3	27.6, CH_3	21.8, CH_3	28.3, CH_3	22.2, CH_3
19	27.6, CH_3	27.7, CH_3	21.5, CH_3	28.2, CH_3	22.0, CH_3	28.5, CH_3
20	13.3, CH_3	13.6, CH_3	13.5, CH_3	13.2, CH_3	13.8, CH_3	14.0, CH_3
21				170.1, C		
22				21.5, CH_3		

[a]125 MHz. [b]200 MHz. [c]175 MHz.

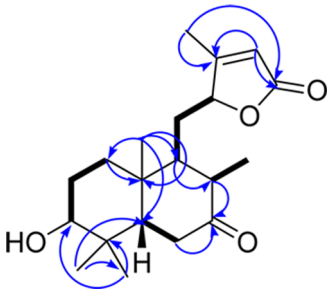

Figure 1. Selected $^1H-^1H$ COSY (bold lines) and HMBC (H→C) correlations of **1**.

Uasdlabdanes B and C (**2** and **3**) had the same molecular formula of $C_{20}H_{30}O_4$, which was deduced from the HRESIMS and ^{13}C NMR data. Analyses of their NMR data (Tables 1 and 2) revealed that both compounds had similar structures to **1**. The ROESY spectra of **2** showed cross-peaks between H-3 (δ_H 3.50)/H_3-18 (δ_H 0.89) and H-5 (δ_H 1.92)/H_3-19 (δ_H 0.96). Crystals of **2** were obtained in MeCN−H_2O, and X-ray crystallography with Cu Kα radiation revealed its absolute configuration as (3*S*, 5*S*, 8*R*, 9*R*, 10*S*, 12*S*) (Figure 2), which was established and confirmed in a similar way to that for **1**.[9−11] Thus, compound **2** was unambiguously identified as an *ent*-labdane diterpenoid and was named uasdlabdane B.

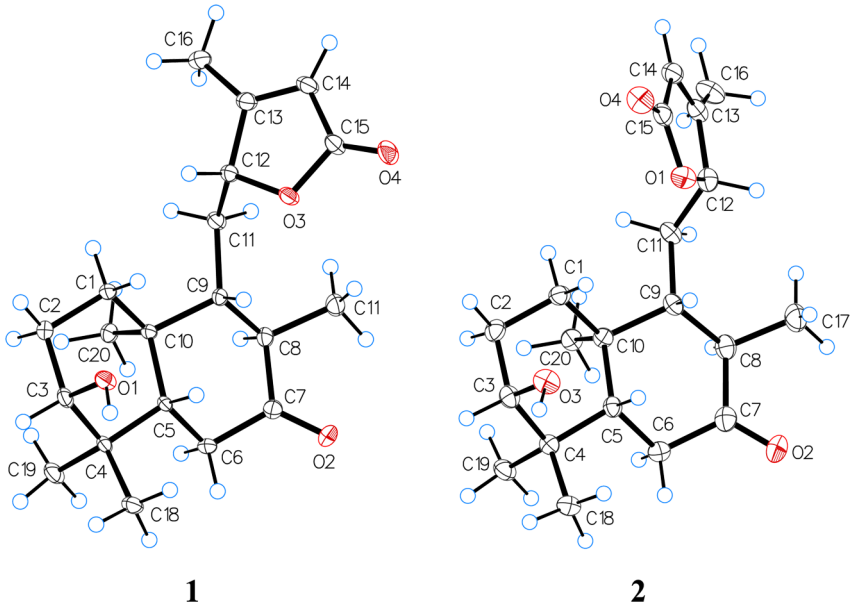

Figure 2. ORTEP drawings of **1** and **2** from X-ray crystallographic data.

DOI: 10.1021/acs.jnatprod.5b00954
J. Nat. Prod. 2016, 79, 907−913

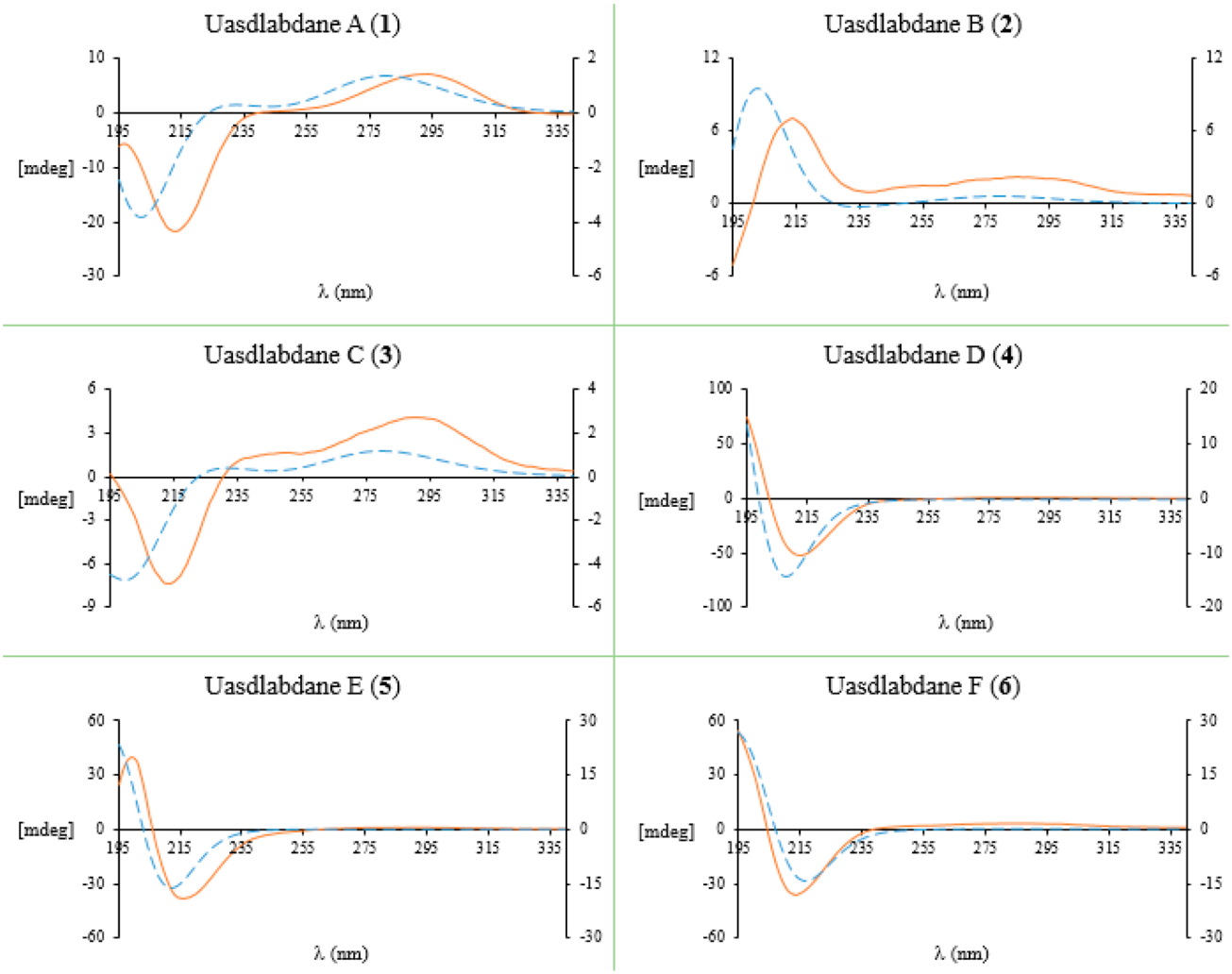

Figure 3. Experimental (solid line) and calculated (dashed line) ECD spectra of compounds **1**−**6**.

A NOESY spectrum of **3** showed, among others, correlations between H-3/H_3-19, H-9/H_3-17, H_3-17/H_3-19, and H_3-18/H_3-20. This suggested that H_3-19 and H_3-20 were on opposite faces of the decalin system, while H-3, H-9, H_3-17, and H_3-19 were cofacial. In order to confirm the relative configuration at C-12, the experimental ECD spectra were recorded for compounds **1**−**6**. In the 200−235 nm region the ECD data of 5-substituted 2(5*H*)-furanones with a stereogenic C-5 show Cotton effects associated with the $\pi\rightarrow\pi^*$ transition, its sign being positive and negative for right-handed (*P*) or left-handed (*M*) helicity of the R−C(5)−C═C bond system, respectively, which implies that 5*S* and 5*R* configured compounds display positive and negative $\pi\rightarrow\pi^*$ Cotton effects, respectively, in that region.[12] Compounds **1** and **3**−**6**, all with the β-oriented H-12, showed a negative Cotton effect (Figure 3), while compound **2**, at the same wavelength region, showed a positive Cotton effect. Thus, the negative Cotton effect experimentally observed for **3**−**6** accounts for a 12*R* absolute configuration. The reliability of this assignment was corroborated by the calculated ECD spectra[13] (Figure 3), which supports the proposed structure for **3**, named uasdlabdane C.

Uasdlabdane D (**4**) exhibited a molecular formula of $C_{22}H_{32}O_5$ based on the ^{13}C NMR and positive-ion HRESIMS (*m*/*z* 399.2170 [M + Na]$^+$, calcd for $C_{22}H_{32}O_5Na$, 399.2147) data, indicating seven indices of hydrogen deficiency. Its ^{1}H and ^{13}C NMR data (Tables 1 and 2) revealed that **4** had a similar chemical structure to **1**−**3**, except for an acetate group at C-7. Additionally, at C-8 the methyl group was replaced by an exocyclic methylene group, a common structural feature found in several labdane diterpenoids.[14−16] The relative configuration of **4** was established through a ROESY experiment, where correlations were observed between H-3/H_3-18, H-5/H-9, H-6α (δ_H 1.63)/H-7, H-6α/H_3-20, and H_3-18/H_3-20. On the basis of these correlations, 3-OH and 7-OAc were cofacial and β-oriented. The configuration of C-12 was defined by analysis of experimental and calculated ECD spectra, which showed a negative Cotton effect in the 200−235 nm region, revealing a 12*R* absolute configuration (Figure 3).[12] Thus, the structure of compound **4** (uasdlabdane D) was defined as shown.

Uasdlabdanes E and F (**5** and **6**) both shared the same molecular formula—$C_{20}H_{30}O_3$—determined by positive-ion HRESIMS and ^{13}C NMR data, suggesting six indices of hydrogen deficiency. NMR data analyses revealed that **5** and **6** had chemical structures similar to **4** but were devoid of the acetate group at C-7. Initially, **5** was considered to be a normal labdane diterpenoid, and its structural elucidation led to the known 3β-hydroxylabda-8(17),13(14)-dien-12(15)-olide, which was reported from *Rauvolfia tetraphylla*.[17] However, comparison of the NMR data with those of **5** revealed the presence of two distinct compounds, based on the large

DOI: 10.1021/acs.jnatprod.5b00954
J. Nat. Prod. 2016, 79, 907−913

Table 3. Antiproliferative Activity (GI_{50}) of Uasdlabdanes A–F (1–6) against Human Solid Tumor Cells[a]

	cell line (origin)					
compound	A549 (lung)	HBL-100 (breast)	HeLa (cervix)	SW1573 (lung)	T-47D (breast)	WiDr (colon)
1	>100	>100	>100	>100	>100	>100
2	>100	>100	>100	>100	>100	>100
3	>100	>100	>100	>100	>100	>100
4	23 (±0.9)	35 (±5.9)	19 (±3.3)	57 (±9.2)	24 (±3.0)	32 (±4.7)
5	59 (±3.4)	>100	62 (±21)	>100	>100	>100
6	44 (±6.6)	>100	62 (±4.1)	>100	>100	>100
etoposide	0.7 (±0.2)	2.3 (±0.9)	3.0 (±0.9)	15 (±1.5)	22 (±5.5)	23 (±2.1)
cisplatin	2.1 (±0.6)	1.9 (±0.2)	2.0 (±0.3)	3.0 (±0.4)	15 (±2.3)	26 (±5.3)

[a]Values are given in μM and are means of two to four experiments; standard deviation is given in parentheses.

differences in the ^{13}C NMR chemical shifts. This observation permitted the conclusion that **5** was an *ent*-labdane and, indeed, a new natural product. A NOESY spectrum of **5** showed correlations between H-3/H_3-19, H-11(δ_H 1.97)/H_3-20, H-11(δ_H 1.86)/H-12, and H_3-18/H_3-20, revealing that H-3 and the C-9 substituent are cofacial, supporting the structure of **5**, which we named uasdlabdane E. The relative configuration of **6** was assigned using a ROESY experiment, where correlations between H-3/H_3-18, H-11(δ_H 1.37)/H_3-20, and H_3-18/H_3-20 were observed. These observations led to the conclusion that H-3 is α-oriented, supporting the structure proposed for **6**, named uasdlabdane F. The absolute configuration of C-12 for compounds **5** and **6** was assigned as 12*R* based on the experimental and calculated ECD spectra (Figure 3).[12]

Assuming that compounds **3**–**6** share the same biosynthetic formation as compounds **1** and **2**, their absolute configurations were assigned as (3*R*, 5*S*, 8*R*, 9*R*, 10*S*, 12*R*) (**3**), (3*S*, 5*S*, 7*S*, 9*S*, 10*R*, 12*R*) (**4**), (3*R*, 5*S*, 9*R*, 10*S*, 12*R*) (**5**), and (3*S*, 5*S*, 9*R*, 10*S*, 12*R*) (**6**) on the basis of the relative configuration of the ring system and the established absolute configuration of C-12.

The antiproliferative activity of compounds **1**–**6** was studied in a panel of six representative human solid tumor cell lines. The results expressed as GI_{50} are given in Table 3. The standard anticancer drugs etoposide and cisplatin were used for comparison. Compound **4** was the most potent compound, with GI_{50} values in the range 19–57 μM against all cell lines. Labdanes **5** and **6** showed antiproliferative activity at a similar level and only against A549 and HeLa cells. Compounds **1**–**3** were inactive (GI_{50} > 100 μM) in all cell lines tested.

From the antiproliferative activity results some preliminary structure–activity relationships may be inferred. A C-7 acetoxy group produces the best antiproliferative activity (**4** vs **5** and **6**), whereas a C-7 carbonyl group causes total loss of activity, as shown for compounds **1**–**3**. The contribution to the biological activity of the methylene group at C-8 or the C-3 configuration cannot be assessed within this small set of compounds. The role of the other stereogenic centers and functional groups on the antiproliferative activity remains to be established.

In summary, six new *ent*-labdane diterpenoids, uasdlabdanes A–F (**1**–**6**), were characterized from the aerial parts of *E. obtusissmum*. The absolute configurations of **1** and **2** were defined via single-crystal X-ray diffraction analyses and those of **3**–**6** by comparison of experimental and calculated ECD spectra. The antiproliferative activity was studied in human solid tumor cell lines, and the results show that, albeit modest, uasdlabdanes A–F might represent a valid scaffold for the development of new antiproliferative compounds. This is the first report of the isolation, identification, and antiproliferative activity of secondary metabolites from *E. obtusissmum*.

EXPERIMENTAL SECTION

General Experimental Procedures. The melting point of **1** was determined with a MEL-TEMP II (Laboratory Devices, USA) and is uncorrected. Optical rotations were measured on an Autopol IV (Rudolph Research Analytical) polarimeter. UV data were recorded using an Agilent Cary 60 UV–vis spectrophotometer. ECD data were collected in CH_3CN (compounds **1**–**4**, **6**) and EtOH (compound **5**) on an AVIV model 215 circular dichroism spectrometer. IR spectra were recorded on an Agilent Cary 630 FTIR spectrometer and a Hyperion 3000 Fourier transform infrared microscope. NMR spectra were acquired on one of three spectrometers: Agilent Direct Drive (VNMRS) 500 and 800 MHz spectrometers with cold probes (the latter was equipped with a carbon-enhanced preamp for ^{13}C spectra and was driven by vnmrj 4.2 software) and a Bruker Avance III 700 MHz spectrometer with a cryoprobe. The chemical shift (δ) values are given in ppm, where the ^1H data are referenced relative to the residual protonated solvent ($CDCl_3$); ^{13}C signals were set internally in the spectrometer relative to tetramethylsilane at 0 ppm. Coupling constants (*J*) are given in Hz. Survey spectra for ^1H and ^{13}C were performed with a 45-degree flip R_f pulse (^1H 90°, 10 μs @ 57db; ^{13}C 90°, μs @ 58 dB) with WALTZ decoupling (^1H decoupling field strength $B_{eff} = \gamma/2\pi B_{1(applied)} \approx 11\,500$ at 500 MHz and 18 519 Hz at 800 MHz). Gradients with adiabatic inversion pulses were used in the heteronuclear experiments when appropriate for COSY, 200–400 ms NOESY, 200–400 ms ROESYAD, gHMBCAD ($^nJ_{xh}$ = 8 Hz), and gHSQCAD ($^1J_{xh}$ = 146 Hz); a ^{13}C adiabatic WURT-40 pulse was used for decoupling experiments with a $B_{eff} = \gamma/2\pi B_{1(applied)}$ of 32 248 Hz. HRESIMS spectra were recorded on an Agilent LC-MS Q-TOF 6540 mass spectrometer and a Bruker Maxis 4G Q-TOF mass spectrometer. Silica gel 60 (particle sizes 0.040–0.063 mm and 0.015–0.040 mm, Merck KGaA, Darmstadt, Germany) was used for column chromatography. Analytical TLCs were developed on silica gel 60 F_{254} plates (Merck KGaA, Darmstadt, Germany). Preparative TLCs were conducted on HPTLC silica gel 60 F_{254} plates (Merck KGaA, Darmstadt, Germany). Semipreparative HPLC was performed on a Shimadzu 10AT instrument equipped with an SPD-10Av detector using Phenomenex (5 μm, 10 mm × 250 mm) Luna $C_{18}(2)$ and Phenomenex (4 μm, 10 mm × 250 mm) RP Synergi-hydro (C_{18}aq) columns with mixtures of H_2O and CH_3CN at various flow rates.

Plant Material. The aerial parts of *E. obtusissmum* were collected in November 2010 in Cabrera, María Trinidad Sánchez Province, Dominican Republic. The plant material was identified by Teodoro Clase, a botanist at Jardín Botánico Nacional "Dr. Rafael Ma. Moscoso", Santo Domingo, Dominican Republic, where a voucher specimen (JBSD 121705) was deposited.

Extraction and Isolation. Aerial parts of *E. obtusissmum* were air-dried and ground to a fine powder. The ground material (372 g) was extracted with 95% EtOH using a Soxhlet apparatus. The resulting crude extract (57 g) was dissolved in 95% EtOH (500 mL) and treated with a 5% $Pb(OAc)_2$ solution (500 mL) to precipitate chlorophyll. After 24 h, the mixture was filtered, concentrated *in vacuo* to remove most of the EtOH, and extracted successively with hexanes (4 × 500 mL) and CH_2Cl_2 (3 × 500 mL). The CH_2Cl_2 residue was washed with 1% aqueous NaCl and dried over anhydrous Na_2SO_4 to yield 4.4 g of

DOI: 10.1021/acs.jnatprod.5b00954
J. Nat. Prod. 2016, 79, 907–913

CH_2Cl_2-soluble extract. This extract was subjected to chromatography (silica gel, 0.040−0.063 mm) and eluted with mixtures of hexanes−EtOAc with increasing polarity to afford 10 fractions (F1−F10). F7 (186 mg) was subjected to chromatography (silica gel, 0.015−0.040 mm) with hexanes−acetone mixtures with increasing polarity to afford 23 subfractions. Subfraction F7-12 (16 mg) afforded **6** (0.5 mg) after semipreparative HPLC (CH_3CN−H_2O, 19−52%, at 4 mL/min, Phenomenex column, 4 μm, 10 mm × 250 mm, RP Synergi-hydro C_{18}aq). Part of fraction 8 (394.6 mg) was subjected to chromatography (silica gel, 0.015−0.040 mm) with hexanes−acetone mixtures with increasing polarity to afford 52 subfractions. Subfraction F8-4 (10.5 mg) afforded **5** (1.0 mg) after preparative TLC (silica gel) using a mixture of Et_2O−EtOAc (7:3). Subfraction F8-10 (13 mg) afforded **2** (0.4 mg) after semipreparative HPLC (CH_3CN−H_2O, 30−60%, at 5 mL/min, Phenomenex column, 4 μm, 10 mm × 250 mm, RP Synergi-hydro C_{18}aq). Fraction 9 (611.4 mg) was subjected to chromatography (silica gel 0.015−0.040 mm) with hexanes−acetone mixtures with increasing polarity to afford 66 fractions. Subfractions F9-10 to F9-14 were combined (149.9 mg) and further separated by semipreparative HPLC [CH_3CN−H_2O, 40%, at 5 mL/min, Phenomenex column, 5 μm, 10 mm × 250 mm, Luna C_{18}(2)] to afford compounds **1** (22 mg) and **4** (0.5 mg). Subfraction F9-20 (7.4 mg) was subjected to semipreparative HPLC (CH_3CN−H_2O, 15−55%, at 4 mL/min, Phenomenex column, 4 μm, 10 mm × 250 mm, RP Synergi-hydro C_{18}aq) to yield compound **3** (0.5 mg).

X-ray Crystallographic Analysis of Compounds 1 and 2. The X-ray diffraction data for compounds **1** and **2** were measured on a Bruker D8 Venture PHOTON 100 CMOS system equipped with a Cu Kα INCOATEC Imus microfocus source (λ = 1.541 78 Å). Indexing was performed using APEX2[18] (difference vectors method). Data integration and reduction were performed using SaintPlus 6.01.[19] Absorption correction was performed by a multiscan method implemented in SADABS.[20] Space groups were determined using XPREP in APEX2.[18] The structures were solved using SHELXS-97[21] (direct methods) and refined using SHELXL-2015[22] (full-matrix least-squares on F^2) through an OLEX2 interface program.[23] All non-hydrogen atoms were refined anisotropically. Hydrogen atoms of the −CH, $-CH_2$, and $-CH_3$ groups were placed in geometrically calculated positions and included in the refinement process using a riding model with isotropic thermal parameters: U_{iso}(H) = 1.2(5) U_{eq}(−CH, $-CH_2$(−CH_3)). Hydrogen atoms of −OH groups were found using a difference Fourier map and were freely refined. For **1**, hydrogen atoms of water molecules were found using a difference Fourier map and refined using SADI and DANG restraints.

X-ray crystal data for ***1****:* $C_{20}H_{32}O_5$ (moiety formula $C_{20}H_{30}O_4$·H_2O), fw 352.45, orthorhombic, crystal size 0.22 × 0.13 × 0.03 mm^3, space group $P2_12_12_1$, a = 7.2954(2) Å, b = 15.3248(3) Å, c = 16.6251(4) Å, V = 1858.70(8) $Å^3$, Z = 4, T = 100.0 K, D_{calcd} = 1.260 g/cm^3, μ = 0.719 mm^{-1}, F(000) = 768.0, reflections collected 22 553 (7.846° ≤ 2θ ≤ 137.936°), independent reflections 3443 (R_{int} = 0.0773, R_{sigma} = 0.0422), final R indexes for $I \geq 2\sigma(I)$, R_1 = 0.0375, wR_2 = 0.0920, final R indexes for all data R_1 = 0.0419, wR_2 = 0.0951, the goodness-of-fit on F^2 is 1.049, the Flack parameter x was 0.07(10), and the Hooft parameter y was 0.05(11). Crystallographic data for **1** have been deposited in the Cambridge Crystallographic Data Center (CCDC) as deposit no. CCDC 1428964.[24] The data can be obtained free of charge from the Cambridge Crystallographic Data Centre via www.ccdc.cam.ac.uk/getstructures.

X-ray crystal data for ***2****:* $C_{20}H_{30}O_4$, fw 334.44, orthorhombic, crystal size 0.08 × 0.05 × 0.04 mm^3, space group $P2_12_12_1$, a = 8.3265(2) Å, b = 12.4915(4) Å, c = 17.0449(5) Å, V = 1772.85(9) $Å^3$, Z = 4, T = 99.99 K, D_{calcd} = 1.253 g/cm^3, μ = 0.684 mm^{-1}, F(000) = 728.0, reflections collected 8468 (8.776° ≤ 2θ ≤ 133.188°), independent reflections 2937 (R_{int} = 0.0402, R_{sigma} = 0.0422), final R indexes for $I \geq 2\sigma(I)$, R_1 = 0.0392, wR_2 = 0.0868, final R indexes for all data R_1 = 0.0493, wR_2 = 0.0918, the goodness-of-fit on F^2 is 1.065, the Flack parameter x was −0.02(15), and the Hooft parameter y was 0.00(16). Crystallographic data for **2** have been deposited in the Cambridge Crystallographic Data Center (CCDC) as deposit no. CCDC 1428963.[24] The data can be obtained free of charge from The Cambridge Crystallographic Data Centre via www.ccdc.cam.ac.uk/getstructures.

Uasdlabdane A ***(1)****:* colorless crystals from CH_3CN−H_2O; mp 171−177 °C; $[\alpha]^{20}_D$ +72 (c 0.1, $CHCl_3$); UV (EtOH) λ_{max} (log ε) 210 (0.41) nm; ECD (CH_3CN) 213 ($\Delta\varepsilon$ −4.44); IR ν_{max} 3499, 2992, 2944, 2925, 2877, 1722, 1700, 1644, 1182, 1067, 851 cm^{-1}; ^1H and ^{13}C NMR data, see Tables 1 and 2; HRESIMS m/z 357.2046 [M + Na]$^+$ (calcd for $C_{20}H_{30}O_4Na$, 357.2042).

Uasdlabdane B ***(2)****:* colorless crystals from CH_3CN−H_2O; $[\alpha]^{24}_D$ +8 (c 0.04, $CHCl_3$); UV (CH_3CN) λ_{max} (log ε) 207 (0.26) nm; ECD (CH_3CN) 214 ($\Delta\varepsilon$ +1.77); IR ν_{max} 3454, 2925, 2858, 1726, 1514, 1461, 1298, 1249, 1160, 1048, 996, 836 cm^{-1}; ^1H and ^{13}C NMR data, see Tables 1 and 2; HRESIMS m/z 335.2217 [M + H]$^+$ (calcd for $C_{20}H_{31}O_4$, 335.2222).

Uasdlabdane C ***(3)****:* oily liquid; $[\alpha]^{24}_D$ +4 (c 0.1, $CHCl_3$); UV (CH_3CN) λ_{max} (log ε) 205 (0.55) nm; ECD (CH_3CN) 214 ($\Delta\varepsilon$ −1.85); IR ν_{max} 3502, 2929, 2873, 1741, 1707, 1648, 1465, 1391, 1305, 1182, 1074, 988, 851, 758, 597 cm^{-1}; ^1H and ^{13}C NMR data, see Tables 1 and 2; HRESIMS m/z 335.2192 [M + H]$^+$ (calcd for $C_{20}H_{31}O_4$, 335.2222).

Uasdlabdane D ***(4)****:* oily liquid; $[\alpha]^{20}_D$ +9 (c 0.1, $CHCl_3$); UV (EtOH) λ_{max} (log ε) 210 (0.46) nm; ECD (CH_3CN) 213 ($\Delta\varepsilon$ −5.92); IR ν_{max} 3514, 3476, 2936, 2877, 1730, 1644, 1376, 1242, 754 cm^{-1}; ^1H and ^{13}C NMR data, see Tables 1 and 2; HRESIMS m/z 399.2170 [M + Na]$^+$ (calcd for $C_{22}H_{32}O_5Na$, 399.2147).

Uasdlabdane E ***(5)****:* oily liquid; $[\alpha]^{23}_D$ +19 (c 0.1, $CHCl_3$); UV (EtOH) λ_{max} (log ε) 219 (1.51) nm; ECD (EtOH) 216 ($\Delta\varepsilon$ −3.71); IR ν_{max} 3302, 2926, 1733, 1642, 1569, 1441, 1385, 1306, 1154, 1049, 985, 903, 844, 600 cm^{-1}; ^1H and ^{13}C NMR data, see Tables 1 and 2; HRESIMS m/z 341.2087 [M + Na]$^+$ (calcd for $C_{20}H_{30}O_3Na$, 341.2093).

Uasdlabdane F ***(6)****:* oily liquid; $[\alpha]^{24}_D$ +8 (c 0.1, $CHCl_3$); UV (CH_3CN) λ_{max} (log ε) 206 (0.42) nm; ECD (CH_3CN) 214 ($\Delta\varepsilon$ −3.51); IR ν_{max} 3469, 2936, 2873, 1763, 1737, 1644, 1447, 1391, 1309, 1160, 1074, 988, 929, 907, 761, 605 cm^{-1}; ^1H and ^{13}C NMR data, see Tables 1 and 2; HRESIMS m/z 301.2136 [M − H_2O + H]$^+$ (calcd for $C_{20}H_{29}O_2$, 301.2168).

Computational Methods. Quantum chemical calculation of ECD was performed with the Gaussian 09W program package[25] revision D.01 using time-dependent density functional theory (TDDFT). For each compound, ECD calculations comprised two steps. First, the geometrical optimization was done to obtain the lowest energy conformer using DFT at the B3LYP/6-31G* level in the gas phase level to confirm minima. Second, for each optimized conformer the excitation energy (in nm) and rotatory strength R (unit: 10^{-40} cgs) in the dipole velocity (R_{vel}) and dipole length (R_{len}) forms were calculated in CH_3CN by TDDFT/B3LYP/6-31G**, using the SCRF method, with the CPCM model. The calculated rotatory strengths are simulated into an ECD curve.

Biological Activity. Cells were inoculated onto 96-well microtiter plates in a volume of 100 μL per well at densities of 2500 (A549, HBL-100, and HeLa) and 5000 (SW1573, T-47D, and WiDr) cells per well, based on their doubling times. Compounds **1**−**6** were initially dissolved in DMSO at 400 times the final maximum test concentration. Control cells were exposed to an equivalent concentration of DMSO (0.25% v/v, negative control). Each compound was tested in triplicate at different dilutions in the range 0.001−100 μM. The drug treatment started on day 1 after plating. Drug incubation times were 48 h, after which cells were precipitated with 25 μL of ice-cold TCA (50% w/v) and fixed for 60 min at 4 °C. Then, the SRB assay was performed.[26] The optical density (OD) of each well was measured at 530 nm, using BioTek's PowerWave XS absorbance microplate reader. Values were corrected for background OD from wells containing only medium. The antiproliferative activity for each compound, expressed as GI_{50} values, was calculated according to NCI formulas.[26]

DOI: 10.1021/acs.jnatprod.5b00954
J. Nat. Prod. 2016, 79, 907−913

■ ASSOCIATED CONTENT

Supporting Information

The Supporting Information is available free of charge on the ACS Publications website at DOI: 10.1021/acs.jnatprod.5b00954.

1D and 2D NMR spectra for compounds **1**−**6** (PDF)

■ AUTHOR INFORMATION

Corresponding Author

*E-mail (Q. A. Castillo): qcastillo55@uasd.edu.do.

Notes

The authors declare no competing financial interest.

■ ACKNOWLEDGMENTS

This research was supported financially by the Ministerio de Educación Superior, Ciencia y Tecnología (MESCYT), Dominican Republic, under grant FONDOCYT 2009-16. Chemical analyses for this work were conducted at the Biointerfaces Institute, McMaster University (Hamilton, Ontario, Canada), and at the USF Interdisciplinary NMR Facility (USFINMRF, Tampa, FL, USA), sponsored by the Department of Chemistry and the Center of Drug Discovery and Innovation at the University of South Florida, CDDI-USF, Tampa, FL, USA. Thanks to USF Mass Spectrometry/Peptide Facility (USFMASP) for the HRESIMS and ECD measurements. L.C. thanks the Ecole Nationale Supérieure de Chimie de Clermont-Ferrand (ENSCCF) for its research internship program. J.M.P. thanks the EU Research Potential (FP7-REGPOT-2012-CT2012-31637-IMBRAIN) and the European Regional Development Fund (FEDER).

■ REFERENCES

(1) Liogier, A. H. *La Flora de la Española. VIII*; Universidad Central del Este: San Pedro de Macorís, 1996; p 142.

(2) Ignea, C.; Ioannou, E.; Georgantea, P.; Loupassaki, S.; Trikka, F. A.; Kanellis, A. K.; Makris, A. M.; Roussis, V.; Kampranis, S. C. *Metab. Eng.* **2015**, *28*, 91−103.

(3) Zhang, M.; Wang, J.; Luo, J.; Wang, P.; Guo, C.; Kong, L. *Fitoterapia* **2013**, *91*, 95−99.

(4) Corlay, N.; Lecsö-Bornet, M.; Leborgne, E.; Blanchard, F.; Cachet, X.; Bignon, J.; Roussi, F.; Butel, M.; Awang, K.; Litaudon, M. *J. Nat. Prod.* **2015**, *78*, 1348−1356.

(5) Zhang, J.; Li, Y.; Zhu, R.; Li, L.; Wang, Y.; Zhou, J.; Qiao, Y.; Zhang, Z.; Lou, H. *J. Nat. Prod.* **2015**, *78*, 2087−2094.

(6) Huang, Z.; Zhu, Z.; Li, Y.; Pang, D.; Zheng, J.; Zhang, Q.; Zhao, Y.; Ferreira, D.; Zjawiony, J. K.; Tu, P.; Li, J. *J. Nat. Prod.* **2015**, *78*, 2276−2285.

(7) Chao, W.; Lin, B. *Chin. Med.* **2012**, *3*, 136−143.

(8) Xu, J.; Liu, C.; Guo, P.; Guo, Y.; Jin, D.; Song, X.; Sun, Z.; Gui, L.; Ma, Y. *Fitoterapia* **2011**, *82*, 772−776.

(9) Flack, H. D. *Acta Crystallogr., Sect. A: Found. Crystallogr.* **1983**, *A39*, 876−881.

(10) Hooft, R. W. W.; Straver, L. H.; Spek, A. L. *J. Appl. Crystallogr.* **2008**, *41*, 96−103.

(11) Spek, A. L. *Acta Crystallogr., Sect. D: Biol. Crystallogr.* **2009**, *D65*, 148−155.

(12) Gawronski, J. K.; Van Oeveren, A.; Van der Deen, H.; Leung, C. W.; Feringa, B. L. *J. Org. Chem.* **1996**, *61*, 1513−1515.

(13) Li, X. C.; Ferreira, D.; Ding, Y. *Curr. Org. Chem.* **2010**, *14*, 1678−1697.

(14) Xiao, P.; Sun, C.; Zahid, M.; Ishrud, O.; Pan, Y. *Fitoterapia* **2001**, *72*, 837−838.

(15) Chokchaisiri, R.; Chaneiam, N.; Svasti, S.; Fucharoen, S.; Vadolas, J.; Suksamrarn, A. *J. Nat. Prod.* **2010**, *73*, 724−728.

(16) Li, D.; Tang, C.; Quinn, R. J.; Feng, Y.; Ke, C.; Yao, S.; Ye, Y. *J. Nat. Prod.* **2013**, *76*, 1580−1585.

(17) Brahmachari, G.; Mandal, L. C.; Gorai, D.; Mondal, A.; Sarkar, S.; Majhi, S. *J. Chem. Res.* **2011**, *35*, 678−680.

(18) Bruker AXS Inc. *APEX2* (Version 2013. 6-2); Madison Publishing House: WI, 2014.

(19) Bruker AXS Inc. *SAINT-V8.32A Data Reduction Software*; Madison Publishing House: WI, 2013.

(20) Sheldrick, G. M. *SADABS Program for Empirical Absorption Correction*; University of Göttingen: Göttingen, Germany, 1996.

(21) Sheldrick, G. M. *Acta Crystallogr., Sect. A: Found. Crystallogr.* **2008**, *64*, 112−122.

(22) Sheldrick, G. M. *Acta Crystallogr.* **2015**, *C71*, 3−8.

(23) Dolomanov, O. V.; Bourhis, L. J.; Gildea, R. J.; Howard, J. A. K.; Puschmann, H. *J. Appl. Crystallogr.* **2009**, *42*, 339−341.

(24) Crystallographic data for compounds **1** and **2** reported in this paper have been deposited with the Cambridge Crystallographic Data Centre. Copies of the data can be obtained, free of charge, upon application to the Director, CCDC, 12 Union Road, Cambridge CB2 1EZ, UK (fax: + 44-(0)1223-336033 or e-mail: deposit@ccdc.cam.ac.uk).

(25) Frisch, M. J.; Trucks, G. W.; Schlegel, H. B.; Scuseria, G. E.; Robb, M. A.; Cheeseman, J. R.; Scalmani, G.; Barone, V.; Mennucci, B.; Petersson, G. A.; Nakatsuji, H.; Caricato, M.; Li, X.; Hratchian, H. P.; Izmaylov, A. F.; Bloino, J.; Zheng, G.; Sonnenberg, J. L.; Hada, M.; Ehara, M.; Toyota, K.; Fukuda, R.; Hasegawa, J.; Ishida, M.; Nakajima, T.; Honda, Y.; Kitao, O.; Nakai, H.; Vreven, T.; Montgomery, J. A., Jr.; Peralta, J. E.; Ogliaro, F.; Bearpark, M. J.; Heyd, J.; Brothers, E. N.; Kudin, K. N.; Staroverov, V. N.; Kobayashi, R.; Normand, J.; Raghavachari, K.; Rendell, A. P.; Burant, J. C.; Iyengar, S. S.; Tomasi, J.; Cossi, M.; Rega, N.; Millam, N. J.; Klene, M.; Knox, J. E.; Cross, J. B.; Bakken, V.; Adamo, C.; Jaramillo, J.; Gomperts, R.; Stratmann, R. E.; Yazyev, O.; Austin, A. J.; Cammi, R.; Pomelli, C.; Ochterski, J. W.; Martin, R. L.; Morokuma, K.; Zakrzewski, V. G.; Voth, G. A.; Salvador, P.; Dannenberg, J. J.; Dapprich, S.; Daniels, A. D.; Farkas, ö.; Foresman, J. B.; Ortiz, J. V.; Cioslowski, J.; Fox, D. J. *Gaussian 09*; Gaussian, Inc.: Wallingford, CT, USA, 2009.

(26) Monks, A.; Scudiero, D.; Skehan, P.; Shoemaker, R.; Paull, K.; Vistica, D.; Hose, C.; Langley, J.; Cronise, P.; Vaigro-Wolff, A.; Gray-Goodrich, M.; Campbell, H.; Boyd, M. *J. Natl. Cancer Inst.* **1991**, *83*, 757−766.

DOI: 10.1021/acs.jnatprod.5b00954
J. Nat. Prod. 2016, 79, 907−913